Effect of Sheet Morphology on the Scalability of Graphene-Based Ultracapacitors

Jiayan Luo,[†] Hee Dong Jang,[†,‡,*] and Jiaxing Huang[†,*]

[†]Department of Materials Science and Engineering, Northwestern University, Evanston, Illinois 60208, United States, and [‡]Rare Metals Research Center, Korea Institute of Geoscience and Mineral Resources, Yuseong-gu, Daejeon 305-350, Korea

ABSTRACT Graphene is considered a promising ultracapacitor material toward high power and energy density because of its high conductivity and high surface area without pore tortuosity. However, the two-dimensional (2D) sheets tend to aggregate during the electrode fabrication process and align perpendicular to the flow direction of electrons and ions, which can reduce the available surface area and limit the electron and ion transport. This makes it hard to achieve scalable device performance as the loading level of the active material increases. Here, we report a strategy to solve these problems by transforming the 2D graphene sheet into a crumpled paper ball structure. Compared to flat or wrinkled sheets, the crumpled graphene balls can deliver much higher specific capacitance and better rate performance. More importantly, devices made with crumpled graphene balls are significantly less dependent on the electrode mass loading. Performance of graphene-based ultracapacitors can be further enhanced by using flat graphene sheets as the binder for the crumpled graphene balls, thus eliminating the need for less active binder materials.

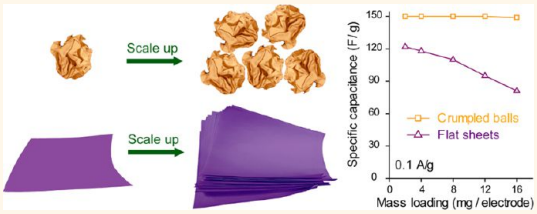

KEYWORDS: aerosol · aggregation · crumpling · graphene · loading level · scalability · ultracapacitor

Bulk quantities of chemically modified graphene can be obtained by first chemically exfoliating graphite powders, followed by reducing the graphite oxide or graphene oxide (GO) product.[1−3] Due to its electrical conductivity and high surface area, chemically modified graphene (aka, reduced GO, r-GO) has attracted significant interest as an electrode material for ultracapacitors.[4−9] While the two-dimensional (2D) shape of graphene is desirable for many of its applications, it actually limits graphene's potential to be fully realized in scaled up ultracapacitor devices. For example, 2D graphene sheets can easily stack to form lamellar microstructures parallel to the current collectors, especially when compressed during electrode preparation. This could affect the device performance adversely in two ways: The effective surface area of the electrodes can be reduced due to aggregation of graphene sheets. The horizontal alignment of the graphene stacks can hinder electron and ion transport since both prefer the direction perpendicular to the current collector. Vertically aligned graphene sheets[10] directly grown on the current collector have been reported and indeed showed outstanding ultracapacitor performance. However, the loading of graphene on the current collector is very limited, which limits overall device capacity and is hard to scale up. Increasing the loading amount of active material is the fundamental step for manufacturing and scaling up devices. Since chemically modified graphene can be made in bulk quantities, to make scalable devices, one would need to solve the aggregation problem so that the device performance does not diminish as the material loading level increases.

The origin of the aggregation is the strong van der Waals attraction between parallel sheets, which scales with the overlapping area (S) and fourth power of the inverse of separating distance between sheets ($1/d^4$).[11] With the high aspect ratio 2D morphology, graphene-based sheets are soft and tend to form conformal contact with a surface or each other, which very effectively increases S and reduces d, thus resulting in strong attraction. To overcome attraction, several general methods have been developed. Within the paradigm of colloidal chemistry,

* Address correspondence to hdjang@kigam.re.kr, jiaxing-huang@northwestern.edu.

Received for review November 11, 2012 and accepted January 25, 2013.

Published online January 27, 2013
10.1021/nn3052378

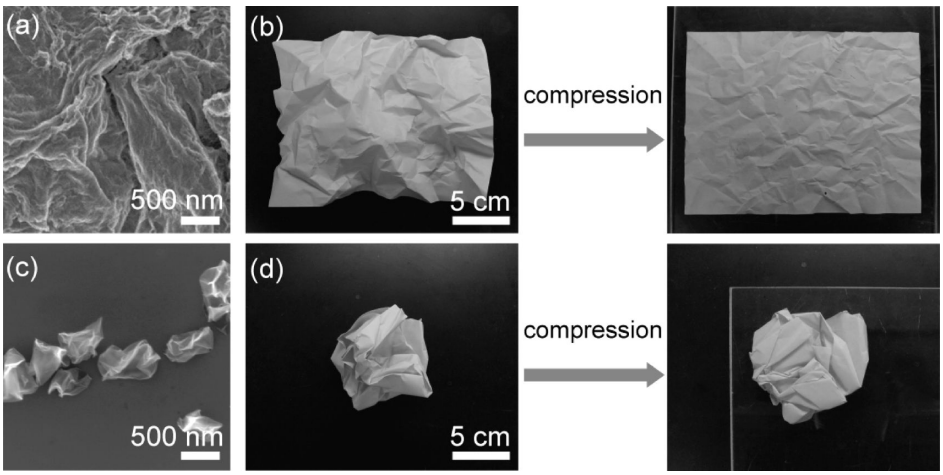

Figure 1. Paper models illustrating the response of (b) heavily wrinkled sheet and (d) crumpled ball being compressed by a glass slide. The wrinkled sheet can be greatly flattened, while the crumpled ball cannot be unfolded, making them aggregation-resistant even after compression. The SEM images on the left column show (a) the surface of heavily wrinkled graphene sheets and (c) crumpled graphene balls.

one can introduce electrostatic repulsion between the sheets by chemically tuning the surface charge of graphene and tailoring the graphene−solvent interactions.[12−14] On the other hand, one can insert molecular or nanostructured spacer materials to prevent the stacking of graphene sheets.[15] However, it is not obvious how these two approaches can alter the orientation of graphene lamella. In an earlier work, we developed an alternative strategy for making graphene resist aggregation by crumpling the 2D sheets into fractal-dimensional paper-ball-like structure.[16] Like paper balls, crumpled graphene balls are remarkably aggregation-resistant. They are dispersible in nearly arbitrary solvents without the need for additional chemical functionalization and remain individually dispersible even after high-pressure compression. Since crumpled graphene balls have more open structure, they have higher specific surface area than the stacked flat sheets. Indeed, we have found that, at the same loading level, the crumpled graphene balls can outperform the flat sheets when they are used as an electrode modifier in microbial fuel cells[16,17] and support for electrocatalysts.[18] Here, we investigate the scalability of graphene-based materials in such electrochemical devices, using ultracapacitors as a model system. Since the near-spherical contour of the crumpled morphology prevents the formation of lamellar structures in compressed graphene pellets, it results in a largely isotropic microstructure for both electron and ion transport. Therefore, this morphology should be more desirable than the flat or even wrinkled sheets for ultracapacitors. As shown below, the aggregation resistance property of the crumpled graphene balls indeed leads to scalable performance of ultracapacitors.

RESULTS AND DISCUSSION

Crumpled GO balls were made by isotropic capillary compression in rapidly evaporating droplets of GO dispersion using an aerosol spray pyrolysis setup.[16,19] The product was collected in a form of fine powders, redispersed in water, and reduced by N_2H_4. For comparison, relatively flat r-GO sheets were synthesized by reducing GO with N_2H_4 under carefully controlled solution pH value, as reported by Li *et al.*[20] Specifically, the GO concentration was kept as low as 0.1 mg/mL, and the pH of the dispersion was tuned to 10 by $NH_3 \cdot H_2O$ before adding a small amount of N_2H_4 to obtained r-GO colloidal solution. Upon slow filtration, a graphene (*i.e.*, r-GO) filter cake was obtained with very ordered lamellar structure. While in such carefully made graphene paper the flat sheets are stacked orderly, in practice, graphene sheets are usually wrinkled after processing and packed rather turbostratically. Therefore, another graphene sample was made by reducing GO in dispersion with much higher concentration (1 mg/mL) with N_2H_4.[21] Agglomeration was observed immediately right after adding N_2H_4. Scanning electron microscopy (SEM) studies reveal that the resulting graphene sheets are heavily wrinkled and deformed during sample processing. It shall be noted that all three samples were treated by N_2H_4 with the same GO/N_2H_4 mass ratio. All three samples were further annealed at 600 °C for 30 min under N_2 before device fabrication. X-ray photoelectron spectroscopy (XPS) (ESCALAB 250Xi) spectra of graphene samples with the three types of morphologies (Figure S1 in the Supporting Information) revealed that hydrazine treatment introduced a small amount of nitrogen (1−2%) into all of the samples. All three types of samples have similar elemental composition.

Wrinkling and crumpling flat paper sheets can prevent them from stacking into dense structures. However, as illustrated by the paper models in Figure 1, since a heavily wrinkled sheet still has a planar contour, it can be largely flattened upon compression along the

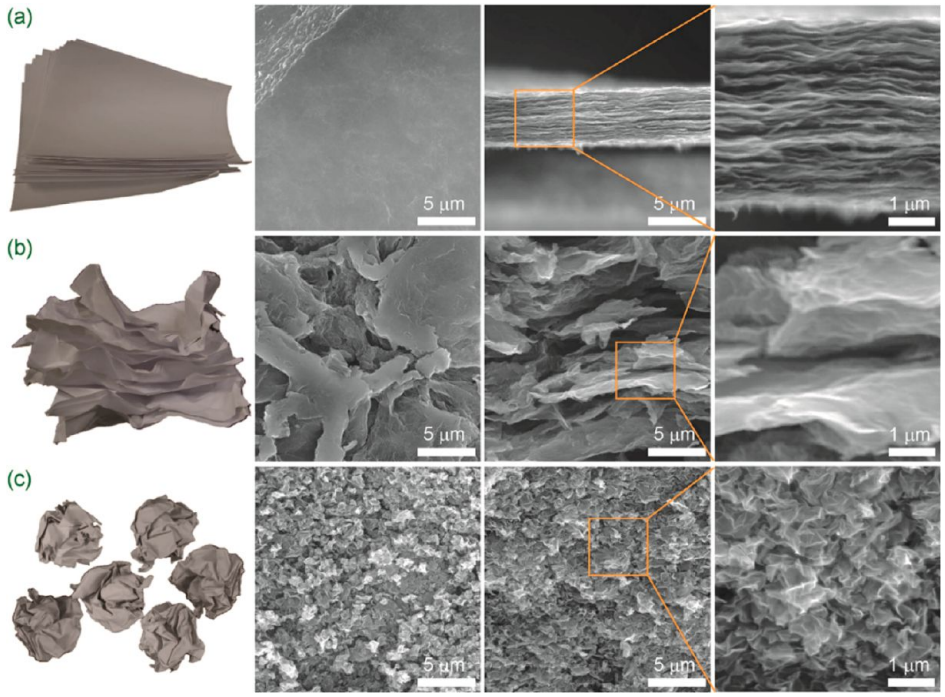

Figure 2. Paper models and SEM images showing stacks of (a) flat graphene sheets, (b) heavily wrinkled sheets, and (c) crumpled graphene balls.

normal direction, thus becoming prone to aggregation again. In contrast, the crumpled ball has a near-spherical contour, thus it can resist compression from any direction without unfolding. In fact, compression will increase the number of folds inside the crumpled ball, making it stiffer and harder to compress.[22] Therefore, to make graphene resist aggregation and sustain the compressive stresses it experiences during material processing, it is necessary to create a structure like the crumpled ball, which has near-spherical contour and can be strain-hardened. How graphene-based materials respond to compression can significantly affect their surface area during processing. For example, as shown in our earlier work,[16] the Brumauer–Emmett–Teller (BET) surface area of wrinkled sheets decreased from 407 to 66 m^2/g after being pelletized, while for crumpled graphene balls with an initial surface area of 567 m^2/g, they still maintained a surface area of 255 m^2/g.

Figure 2 shows the microstructures of mechanically compressed pellets of stacked graphene materials of the three different morphologies along with the corresponding paper models. For each sample, SEM images were taken at both the surface and cross section. As expected, the flat graphene sheets pack like a stack of paper with a smooth featureless surface and an ordered lamellar cross section (Figure 2a). For the pellet of wrinkled sheets (Figure 2b), the surface is uneven with many micrometer-sized flattened islands. The cross sectional view in Figure 2b reveals a largely lamellar but significantly more disordered microstructure. There are many flakes of aggregated graphene sheets, but the flakes themselves do not tightly pack due to uneven size distribution and orientations. This leads to pocket-like void space in the pellet, which decreases the overall density. For the crumpled balls (Figure 2c), the morphology of individual particles in the compressed pellet was largely unchanged. The surface and the cross section have essentially indistinguishable microstructures. It shall be noted that there is free space inside each individual crumpled ball as well as between them. So the pellet of crumpled balls should be less dense than that of the flat sheets. Indeed, the densities of the three types of pellets were measured to be around 1 g/cm^3 for flat sheets and 0.5 g/cm^3 for both wrinkled sheets and crumpled balls. Although the pellets of wrinkled sheets and crumpled balls have similar density, they have very different types of free volume. The former has large, segregated voids, and the latter has much smaller voids uniformly distributed inside and between the particles throughout the pellet, which should be more favorable for the ionic flow and electron transport for ultracapacitor electrodes.

To evaluate the performance of the three graphene samples as ultracapacitor electrodes, two-electrode symmetric coin cells were assembled.[5,23] Aqueous solution of 5 M KOH was used as electrolyte to avoid the pseudocapacitance arising from the oxygenated functional groups in acidic or neutral electrolytes or capacitance decay.[24] The electrode loading level was varied from 2 to 16 mg per electrode (~0.8 cm^2). We used CR2016 coin cells in our experiments, which have an apparent thickness of 1.6 mm. In such cells, 16 mg of crumpled graphene particles would fill up to a height

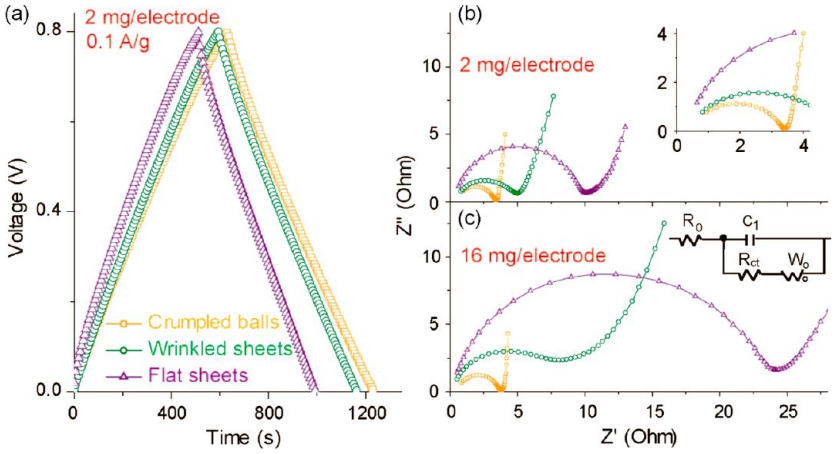

Figure 3. (a) Typical charge/discharge curves of symmetric ultracapacitor devices at 0.1 A/g using crumpled graphene balls, wrinkled graphene sheets, and flat sheets as electrodes. Nyquist plots of the three samples with mass loading of (b) 2 mg and (c) 16 mg per electrode. The inset of (b) shows the zoom-in view of the intersections with the Z' axis showing the ohmic resistance of the devices. The inset of (c) shows an equivalent circuit of the devices. The morphology has little effect on the ohmic resistance but greatly affects the charge transfer resistance and diffusion resistance, especially at higher mass loading.

about 0.4 mm. This is close to the maximal loading level of graphene for a single electrode in the cell since the separator and the stainless steel current collectors also occupy some space. Galvanostatic constant current charge/discharge method was used to determine the specific capacitance of the materials. Typical charge/discharge curves of symmetric ultracapacitor devices using crumpled graphene balls, wrinkled graphene sheets, and flat sheets as electrodes active materials are shown in Figure 3a. All of the curves display isosceles triangle shape without plateaus, illustrating the electrochemical double-layer capacitance behaviors of the three graphene materials. The Coulombic efficiency for all three samples was close to 100% in the test voltage range. The capacitance value for the three samples was stable upon a few thousand charge/discharge cycles (*ca.* 4 min per cycle) without appreciable degrading. It should be noted that the electrodes made with flat or wrinkled graphene sheets were binder-free. Since the crumpled graphene balls are aggregation-resistant, 10 wt % of PTFE binder was added to maintain the mechanical integrity of the crumpled graphene electrode. With these prerequisites, the morphology effect on the performance can be pursued. The specific capacitance based on the mass of graphene was calculated to be 150, 141, and 122 F/g for crumpled graphene balls, wrinkled, and flat graphene sheets, respectively, when they were tested under 0.1 A/g with a loading level of 2 mg/electrode (Figure 3a).

Electrochemical impedance spectroscopy (EIS) was used to study the electron and ion transport in the three graphene electrodes.[25] The EIS measurements were recorded over the frequency range of 1000−0.01 Hz with AC oscillation voltage of 5 mV around open circuit voltage with mass loading of 2 mg (Figure 3b) and 16 mg (Figure 3c) per electrode, respectively. An equivalent circuit is shown in the inset of Figure 3c. The first intersections of the curves with the real axis at high frequency indicate the ohmic resistance R_o of the ultracapacitor, which includes the intrinsic resistance of the electrode materials, the electrolyte, and the contact resistance between the interfaces of electrodes, electrolyte, and current collector substrates. The morphological difference in graphene has little effect on the ohmic resistance of the ultracapacitor device, as shown in the zoom-in of the intersection part (Figure 3b inset). However, the morphology plays a significant role in the charge transfer, as shown in the high to medium frequency semicircle regions. Typically, the smaller radii of the semicircles, the lower resistance of charge transfer R_{ct}. Changing the morphology of graphene from flat sheets, wrinkled sheets to crumpled balls decreases the radius of the semicircles, indicating that the charge transfer process is facilitated by the 3D porous structure in the crumpled graphene electrode (Figure 3b). The advantage becomes more apparent for thicker electrodes. For example, increasing the mass loading from 2 to 16 mg per electrode raises the R_{ct} of the wrinkled and flat sheets by 80 and 140%, respectively, but only 10% for the crumpled graphene balls (Figure 3c). The 2D layered structure was also found to restrain the electrolyte diffusion into the bulk electrodes, reflected by the slope of the tails extending beyond the semicircle in the low frequency region. If there is no diffusion resistance R_w, the tails should be vertical lines normal to the real axis. Flatter graphene sheets tend to stack horizontally on the current collector, resulting in higher ion diffusion resistance and thus smaller slopes of the tails. Cyclic voltammetry curves at 20 mV/s of devices made from flat sheets, wrinkled sheets and crumpled balls show the polarization of the three samples (Figure S2), and the voltage drop is illustrated by the charge/

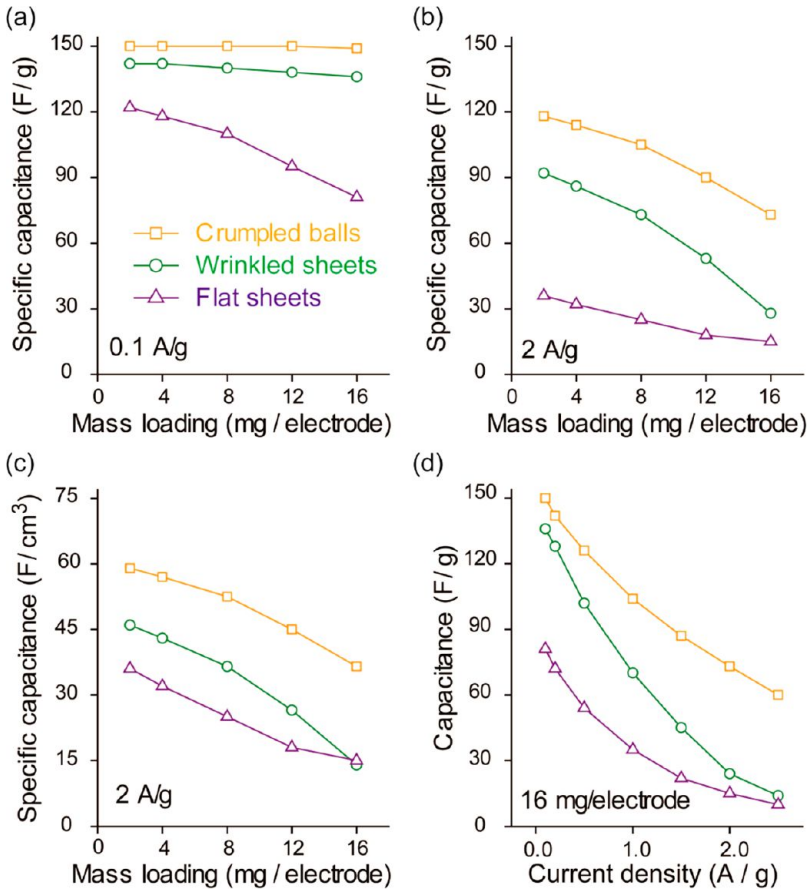

Figure 4. Mass-based specific capacitance of the three graphene samples as a function of mass loading at current density of (a) 0.1 and (b) 2 A/g. (c) Volumetric specific capacitance of the three graphene electrodes at 2 A/g. (d) Mass-based specific capacitance of the three graphene samples as a function of current density with mass loading of 16 mg/electrode.

discharge curves at high current rate of 1A/g (Figure S3), both of which are in agreement with impedance results.

The loading level of active materials in an ultracapacitor should be scalable to achieve high energy density for the whole device. However, with increased electrode thickness, the ion and electron transport distance/resistance in the electrodes will increase and thus decrease the specific capacitance of materials, especially at high charge/discharge rate.[26−28] This conflict becomes more serious when it comes to graphene-based materials, as the orientation of high aspect ratio graphene sheets tends to align perpendicularly to the direction of ion and electron field. Figure 4a shows that, at a low current rate of 0.1 A/g, the specific capacitance of flat graphene sheets decreases from 122 to 81 F/g when the electrode loading increases from 2 to 16 mg. Under the same testing conditions, the specific capacitance of wrinkled sheets deceased from 142 to 136 F/g. However, the specific capacitance of the crumpled graphene balls was stable around 150 F/g. As shown in Figure 4b, the effect of electrode thickness (*i.e.*, mass loading level) becomes more apparent at high current rate. At current density of 2 A/g, only 36 F/g was delivered from flat graphene sheets at a mass loading level of 2 mg per electrode, which decreased to 15 F/g when the mass of graphene increased to 16 mg per electrode. The wrinkled graphene sheets displayed relative high capacitance of 92 F/g at low loading level, which rapidly decreased to 28 F/g at high loading level. The crumpled graphene balls delivered specific capacitance of 118 F/g at low loading level yet still delivered 73 F/g at 16 mg per electrode. Figure 4a,b shows that crumpled graphene balls significantly outperform wrinkled or flat graphene sheets, especially at high current density and high mass loading level. Note that usually specific capacitance is based on mass; however, volumetric specific capacitance is also important as it determines the form factor of the device. The density of the bulk solid of flat, wrinkled, and crumpled graphene was found to be around 1, 0.5, and 0.5 g/cm^3, respectively. The mass-based specific capacitances in Figure 4b can be converted to volumetric specific capacitance, which is shown in Figure 4c. It shows that, at high current density, the crumpled graphene balls also have the highest volumetric specific capacitance. It shall be noted that the densities of these three graphene samples are comparable to those of activated carbon or mesoporous carbon.[29] Although three-dimensional graphene foams can also increase the surface area[30,31] and at same time resist aggregation, they usually have

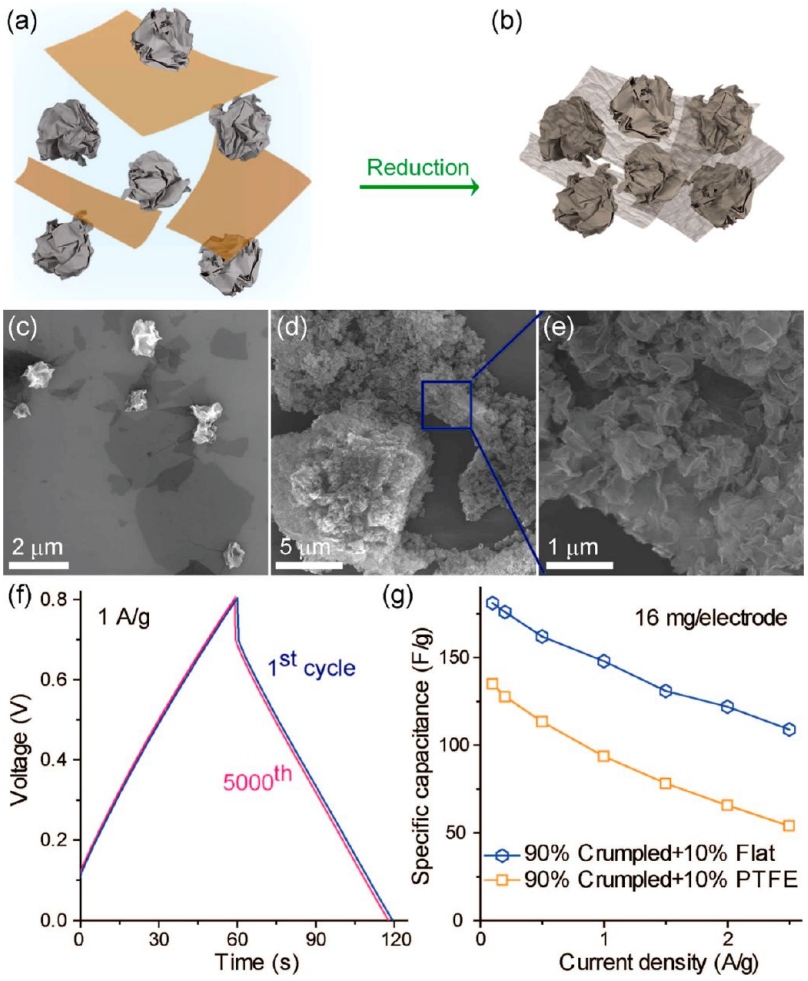

Figure 5. Uncrumpled graphene sheets as binder for the crumpled graphene balls. (a) Schematic drawings showing GO is used to disperse crumpled graphene balls in aqueous dispersion, followed by (b) reduction to obtain the composite with mixed morphologies. (c) SEM image showing crumpled graphene particles adhering to GO sheets before reduction. (d,e) SEM image of the agglomerates obtained after reducing GO, revealing tight binding between the two morphologies. (f) First and 5000th charge/discharge curves at 1A/g of a symmetric ultracapacitor device using the composite as electrodes. (g) Specific capacitance (based on the total mass of the electrodes) of the flat/crumpled graphene composites as a function of current density compared to that of crumpled graphene electrode using the PTFE binder.

very low density, which could limit the volumetric-based device performance.

Figure 4d summarizes the current density effect on the three graphene samples at the highest loading level of 16 mg per electrode. The specific capacitance deceases from 150 to 60, 136 to 14, and 81 to 10 F/g, respectively, for crumpled graphene balls, wrinkled, and flat sheets when the current density increased from 0.1 to 2.5 A/g. Ragone plot calculated from Figure 4d of the three graphene samples is shown in Figure S4. It is interesting to note that, in terms of specific capacitance, the performance of wrinkled sheets is nearly as good as that of the crumpled balls at low current density but rapidly degrades to be as poor as that of the flat sheets at high current density. The observation is consistent with the aggregation properties of wrinkled sheets: they can resist aggregation without much compression (*i.e.*, low mass loading level), but they can be flattened under pressure (*i.e.*, high mass loading level) and aggregate like flat sheets. At low current rates, sufficient time is allowed for the electron and ions to transport through the aggregated stacks of wrinkled sheets, which are greatly hindered at high current rates.

On the basis of the above results, transforming the 2D graphene sheets to the aggregation-resistant crumpled ball morphology is favorable for achieving scalable ultracapacitor performance in terms of electrode mass loading. The aggregation-resistant property of crumpled graphene balls brings significant advantages leading to more scalable device performance. However, this property also makes it difficult to bind the particles together to form a continuous solid. As mentioned earlier, binder materials are needed for fabricating electrodes of crumpled graphene particles. The PTFE binder is inactive, insulating, and may not be well wetted by the electrolytes.[32] In addition, the PTFE particles are around tens of nanometers, which can be

pushed into the openings of the crumpled graphene balls, thus hindering electrolyte access. We noted that the flat and wrinkled graphene sheets can form binder-free electrodes. Therefore, the crumpled graphene balls could be connected together using their flat counterparts as the binder. Although the crumpled graphene balls do not stick to each other permanently, they can adhere to the flat GO sheets, likely through $\pi-\pi$ interaction (Figure 5a,c). This is consistent with our earlier discovery that GO can act as colloidal surfactant to disperse carbon nanotubes or graphite powders in water.[33−35] To make a crumpled graphene electrode with uncrumpled graphene as the binder, the crumpled particles were first dispersed with GO sheets in water (Figure 5a). After reducing the GO sheets (Figure 5b), large agglomerates about 10 μm in size were observed, which contain a uniform mixture of sheet-bound crumples, as revealed by the SEM images (Figure 5b,d,e). The starting mass ratio of GO sheets to crumpled graphene was set to be 25:90. Since GO loses approximately 50−60% of its mass after reduction,[36] the mass ratio of flat/crumpled graphene should be around 10:90. Assuming there are 15−30 graphene layers in a typical crumpled particle,[16] the uncrumpled binder sheets should outnumber the crumpled graphene particles by 2−3 times. Therefore, there should be sufficient binder for establishing robust connections between the crumpled particles. Indeed, charge/discharge cycling tests at 1A/g of a symmetric ultracapacitor made of the uncrumpled/crumpled graphene hybrid showed that its specific capacitance remained the same after 5000 cycles (*ca.* 4 min per cycle, Figure 5f). Specific capacitance of the flat/crumpled graphene hybrid was measured to be 181 F/g at low current density of 0.1 A/g, compared with 135 F/g (based on the mass of both graphene and binder) for the crumpled graphene/PTFE composite (Figure 5g). With the current density increased to 2.5 A/g, the flat/crumpled graphene composite could still maintain 60% of its specific capacitance at 0.1 A/g, compared with 40% for the graphene/PTFE composite.

CONCLUSION

In conclusion, converting flat graphene sheets into crumpled paper-ball-like morphology can significantly improve the scalability of graphene-based ultracapacitors. The aggregation-resistant properties of the crumpled particles allow them to maintain high accessible surface area and thus high specific capacitance. The uniformly distributed free space inside and between the crumpled particles can facilitate charge transport, especially at high current density and high mass loading, leading to high specific capacitance and rate capability based on both mass and volume. Using uncrumpled graphene sheets as binder for the crumpled particles eliminates the need for commonly used inactive binder materials such as PTFE colloids and can further improve device performances. The advantages of crumpled paper-ball-like morphology demonstrated here should be transferrable to other devices, applications, and graphene-based composites relying on high surface area of graphene. Therefore, the crumpled graphene particles should be a manufacturable form of graphene allowing scalable and reproducible production of new materials and devices.

MATERIALS AND METHODS

Synthesis of Flat Graphene Sheets, Wrinkled Sheets, and Crumpled Balls. GO was prepared by a modified Hummers' method[37] with an improved purification method as reported elsewhere.[36,38] Crumpled GO particles were prepared by an aerosol spray drying process as reported earlier.[16] Flat graphene sheets were prepared by treating 0.1 mg/mL GO aqueous solution with N_2H_4 (mass ratio N_2H_4/GO = 10:1) under pH 10 adjusted by NH_3H_2O (25%) at 80 °C for 24 h.[20] The resulting dispersion was decanted and vacuum filtrated on anodic aluminum oxide filter membrane (Waterman). Wrinkled graphene sheets and crumpled graphene balls were prepared by reduction of the corresponding GO precursors in aqueous dispersion (1 mg/mL) with N_2H_4 (mass ratio N_2H_4/GO = 10:1) without tuning pH. The resulting graphene (*i.e.*, r-GO) particles were filtered and collected. All three graphene products were then annealed at 600 °C under N_2 for 30 min. The uncrumpled/crumpled graphene composite was prepared by first dispersing the crumpled particles with GO in water (mass ratio of GO sheet/crumpled graphene = 25:90), followed by the same GO reduction and annealing procedures.

Electrochemical Test. The electrochemical behavior of the three graphene samples was characterized by constant current charge/discharge and impedance measurements with two symmetric electrodes in CR2016-type coin cell using an Autolab electrochemical interface instrument (PGSTAT 302N). Flat graphene paper was used for electrodes as-is by cutting an area of ~0.8 cm^2 and then stacked to achieve a mass loading level from 2 to 16 mg per electrode. Wrinkled sheets or the uncrumpled/crumpled graphene composite were dispersed in water with a concentration of 10 mg/mL and drop casted on stainless steel current collectors (0.8 cm^2) to achieve a mass loading from 2 to 16 mg without using binder. Electrodes of crumpled graphene particles were made the same way except that PTFE binder (mass ratio, crumpled graphene/PTFE = 9:1) was added to the dispersion. KOH solution (5 M) was used as the electrolyte, and a filter paper (Waterman, grade no. 4) was used as the separator.

Conflict of Interest: The authors declare no competing financial interest.

Acknowledgment. The authors thank the Initiative for Sustainability and Energy at Northwestern (ISEN) for an Early Career Investigator Award, a gift donation from the Sony Corporation and a Sloan Research Fellowship (J.H.), partial support from a 3M graduate fellowship, a Ryan Fellowship from Northwestern and the Northwestern University International Institute for Nanotechnology (J.L), and the General Research Project of the Korea Institute of Geoscience and Mineral Resources (KIGAM) funded by the Ministry of Knowledge Economy of Korea (J.H. and H.D.J.).

Supporting Information Available: XPS spectra of the flat, wrinkled, and crumpled graphene samples (Figure S1), cyclic voltammetry curves (Figure S2), additional charge/discharge curves (Figure S3), and the Ragone plot of devices made by the crumpled graphene balls, wrinkled, and flat graphene sheets

(Figure S4). This material is available free of charge *via* the Internet at http://pubs.acs.org.

REFERENCES AND NOTES

1. Park, S.; Ruoff, R. S. Chemical Methods for the Production of Graphenes. *Nat. Nanotechnol.* **2009**, *4*, 217–224.
2. Li, D.; Kaner, R. B. Graphene-Based Materials. *Science* **2008**, *320*, 1170–1171.
3. Compton, O. C.; Nguyen, S. T. Graphene Oxide, Highly Reduced Graphene Oxide, and Graphene: Versatile Building Blocks for Carbon-Based Materials. *Small* **2010**, *6*, 711–723.
4. Vivekchand, S. R. C.; Rout, C. S.; Subrahmanyam, K. S.; Govindaraj, A.; Rao, C. N. R. Graphene-Based Electrochemical Supercapacitors. *J. Chem. Sci.* **2008**, *120*, 9–13.
5. Stoller, M. D.; Park, S. J.; Zhu, Y. W.; An, J. H.; Ruoff, R. S. Graphene-Based Ultracapacitors. *Nano Lett.* **2008**, *8*, 3498–3502.
6. Liu, C. G.; Yu, Z. N.; Neff, D.; Zhamu, A.; Jang, B. Z. Graphene-Based Supercapacitor with an Ultrahigh Energy Density. *Nano Lett.* **2010**, *10*, 4863–4868.
7. Yang, X. W.; Zhu, J. W.; Qiu, L.; Li, D. Bioinspired Effective Prevention of Restacking in Multilayered Graphene Films: Towards the Next Generation of High-Performance Supercapacitors. *Adv. Mater.* **2011**, *23*, 2833–2838.
8. Zhu, Y. W.; Murali, S.; Stoller, M. D.; Ganesh, K. J.; Cai, W. W.; Ferreira, P. J.; Pirkle, A.; Wallace, R. M.; Cychosz, K. A.; Thommes, M.; *et al.* Carbon-Based Supercapacitors Produced by Activation of Graphene. *Science* **2011**, *332*, 1537–1541.
9. El-Kady, M. F.; Strong, V.; Dubin, S.; Kaner, R. B. Laser Scribing of High-Performance and Flexible Graphene-Based Electrochemical Capacitors. *Science* **2012**, *335*, 1326–1330.
10. Miller, J. R.; Outlaw, R. A.; Holloway, B. C. Graphene Double-Layer Capacitor with AC Line-Filtering Performance. *Science* **2010**, *329*, 1637–1639.
11. Brennan, R. O. The Interlayer Binding in Graphite. *J. Chem. Phys.* **1952**, *20*, 40–48.
12. Eda, G.; Chhowalla, M. Chemically Derived Graphene Oxide: Towards Large-Area Thin-Film Electronics and Optoelectronics. *Adv. Mater.* **2010**, *22*, 2392–2415.
13. Allen, M. J.; Tung, V. C.; Kaner, R. B. Honeycomb Carbon: A Review of Graphene. *Chem. Rev.* **2010**, *110*, 132–145.
14. Huang, X.; Qi, X. Y.; Boey, F.; Zhang, H. Graphene-Based Composites. *Chem. Soc. Rev.* **2012**, *41*, 666–686.
15. Yu, D. S.; Dai, L. M. Self-Assembled Graphene/Carbon Nanotube Hybrid Films for Supercapacitors. *J. Phys. Chem. Lett.* **2010**, *1*, 467–470.
16. Luo, J. Y.; Jang, H. D.; Sun, T.; Xiao, L.; He, Z.; Katsoulidis, A. P.; Kanatzidis, M. G.; Gibson, J. M.; Huang, J. X. Compression and Aggregation-Resistant Particles of Crumpled Soft Sheets. *ACS Nano* **2011**, *5*, 8943–8949.
17. Xiao, L.; Damien, J.; Luo, J. Y.; Jang, H. D.; Huang, J. X.; He, Z. Crumpled Graphene Particles for Microbial Fuel Cell Electrodes. *J. Power Sources* **2012**, *208*, 187–192.
18. Jang, H. D.; Kim, S. K.; Chang, H.; Choi, J.-W.; Luo, J.; Huang, J. One Step Synthesis of Pt-Nanoparticles-Laden Graphene Crumples by Aerosol Spray Pyrolysis and Evaluation of Their Electrocatalytic Activity. *Aerosol Sci. Technol.* **2013**, *47*, 93–98.
19. Jang, H. D.; Chang, H.; Cho, K.; Kim, F.; Sohn, K.; Huang, J. X. Co-assembly of Nanoparticles in Evaporating Aerosol Droplets: Preparation of Nanoporous Pt/TiO_2 Composite Particles. *Aerosol Sci. Technol.* **2010**, *44*, 1140–1145.
20. Li, D.; Muller, M. B.; Gilje, S.; Kaner, R. B.; Wallace, G. G. Processable Aqueous Dispersions of Graphene Nanosheets. *Nat. Nanotechnol.* **2008**, *3*, 101–105.
21. Stankovich, S.; Dikin, D. A.; Piner, R. D.; Kohlhaas, K. A.; Kleinhammes, A.; Jia, Y.; Wu, Y.; Nguyen, S. T.; Ruoff, R. S. Synthesis of Graphene-Based Nanosheets *via* Chemical Reduction of Exfoliated Graphite Oxide. *Carbon* **2007**, *45*, 1558–1565.
22. Matan, K.; Williams, R. B.; Witten, T. A.; Nagel, S. R. Crumpling a Thin Sheet. *Phys. Rev. Lett.* **2002**, *88*, 076101.
23. Stoller, M. D.; Stoller, S. A.; Quarles, N.; Suk, J. W.; Murali, S.; Zhu, Y. W.; Zhu, X. J.; Ruoff, R. S. Using Coin Cells for Ultracapacitor Electrode Material Testing. *J. Appl. Electrochem.* **2011**, *41*, 681–686.
24. Frackowiak, E.; Beguin, F. Carbon Materials for the Electrochemical Storage of Energy in Capacitors. *Carbon* **2001**, *39*, 937–950.
25. Harrington, D. A.; Conway, B. E. AC Impedance of Faradaic Reactions Involving Electrosorbed Intermediates 0.1. Kinetic-Theory. *Electrochim. Acta* **1987**, *32*, 1703–1712.
26. Hu, L. B.; Choi, J. W.; Yang, Y.; Jeong, S.; La Mantia, F.; Cui, L. F.; Cui, Y. Highly Conductive Paper for Energy-Storage Devices. *Proc. Natl. Acad. Sci. U.S.A.* **2009**, *106*, 21490–21494.
27. Long, J. W.; Dunn, B.; Rolison, D. R.; White, H. S. Three-Dimensional Battery Architectures. *Chem. Rev.* **2004**, *104*, 4463–4492.
28. Toupin, M.; Brousse, T.; Belanger, D. Influence of Microstucture on the Charge Storage Properties of Chemically Synthesized Manganese Dioxide. *Chem. Mater.* **2002**, *14*, 3946–3952.
29. Zhang, L. L.; Zhou, R.; Zhao, X. S. Graphene-Based Materials as Supercapacitor Electrodes. *J. Mater. Chem.* **2010**, *20*, 5983–5992.
30. Xu, Y. X.; Wu, Q. O.; Sun, Y. Q.; Bai, H.; Shi, G. Q. Three-Dimensional Self-Assembly of Graphene Oxide and DNA into Multifunctional Hydrogels. *ACS Nano* **2010**, *4*, 7358–7362.
31. Sheng, K.; Sun, Y.; Li, C.; Yuan, W.; Shi, G. Ultrahigh-Rate Supercapacitors Based on Eletrochemically Reduced Graphene Oxide for AC Line-Filtering. *Sci. Rep.* **2012**, *2*, 247.
32. Luo, J.; Tung, V. C.; Jang, H. D.; Huang, J. Graphene Oxide Based Conductive Glue as Binder for Ultracapacitor Electrodes. *J. Mater. Chem.* **2012**, *22*, 12993–12996.
33. Kim, J.; Cote, L. J.; Kim, F.; Yuan, W.; Shull, K. R.; Huang, J. X. Graphene Oxide Sheets at Interfaces. *J. Am. Chem. Soc.* **2010**, *132*, 8180–8186.
34. Cote, L. J.; Kim, J.; Tung, V. C.; Luo, J. Y.; Kim, F.; Huang, J. X. Graphene Oxide as Surfactant Sheets. *Pure Appl. Chem.* **2011**, *83*, 95–110.
35. Tung, V. C.; Huang, J. H.; Tevis, I.; Kim, F.; Kim, J.; Chu, C. W.; Stupp, S. I.; Huang, J. X. Surfactant-Free Water-Processable Photoconductive All-Carbon Composite. *J. Am. Chem. Soc.* **2011**, *133*, 4940–4947.
36. Krishnan, D.; Kim, F.; Luo, J.; Cruz-Silva, R.; Cote, L. J.; Jang, H. D.; Huang, J. Energetic Graphene Oxide: Challenges and Opportunities. *Nano Today* **2012**, *7*, 137–152.
37. Hummers, W. S.; Offeman, R. E. Preparation of Graphitic Oxide. *J. Am. Chem. Soc.* **1958**, *80*, 1339–1339.
38. Kim, F.; Luo, J. Y.; Cruz-Silva, R.; Cote, L. J.; Sohn, K.; Huang, J. X. Self-Propagating Domino-like Reactions in Oxidized Graphite. *Adv. Funct. Mater.* **2010**, *20*, 2867–2873.